Presented at the 165th American Society
Meeting on Analytical Methods Applied to
Air Pollution Measurements, Dallas,
Texas, April 8-13, 1973

LBL-1743
c.1

APPLICATION OF X-RAY FLUORESCENCE TECHNIQUES TO MEASURE ELEMENTAL COMPOSITION OF PARTICLES IN THE ATMOSPHERE

Joseph M. Jaklevic, Fred S. Goulding,
Blair V. Jarrett and John D. Meng

July 1973

Prepared for the U.S. Atomic Energy Commission
under Contract W-7405-ENG-48

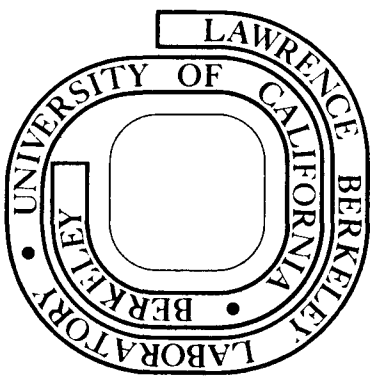

LBL-1743
c.1

DISCLAIMER

APPLICATION OF X-RAY FLUORESCENCE TECHNIQUES TO MEASURE ELEMENTAL COMPOSITION OF PARTICLES IN THE ATMOSPHERE*

Joseph M. Jaklevic, Fred S. Goulding, Blair V. Jarrett and John D. Meng

Lawrence Berkeley Laboratory, University of California
Berkeley, California 94720

ABSTRACT

The design and operation of a system for the automated X-ray fluorescence analysis of atmospheric particulates on filters will be described. Central to the system is a low-background Si(Li) semiconductor detector coupled to a low-power variable-energy X-ray tube used to generate monoenergetic photons for fluorescence excitation. Sequencing of the filter analysis, changes in X-ray excitation energy and intensity, together with data storage can be performed without operator intervention under the control of a small dedicated computer. Reduction of pulse height data and intensity calibration can be performed in real-time in this same computer. The three analysis required to cover over 30 elements can be performed in a total time of one-half hour with detection limits in the worst case of 25 ng/cm^2 or less over filter areas of 7 cm^2. A single analysis for a restricted group of 15 elements at a detection level below 10 ng/cm^2 can be performed in ten minutes. Samples are generated using a fully automated remote sampling station designed for the unattended collecting of up to 30 filter samples using a variety of commercially available filtering materials. The accuracy and sensitivity of the method compared to other sampling and analysis techniques will be discussed.

---

* Work support in part by the Environmental Protection Agency under Interagency Agreement with the U. S. Atomic Energy Commission Contract No. EPA-IAG-0089(D)/A.

INTRODUCTION

X-ray fluorescence is an analytical technique in many ways ideally suited for the routine elemental analysis of atmospheric particulates. The good sensitivity, accuracy and speed, combined with low cost per analysis make it more than competitive with other available methods in applications involving large numbers of samples. A typical sample consists of a uniform deposit of small particles (<100 μm diameter) collected on a clean filter backing. This is almost an ideal thin specimen and permits accurate calibration of X-ray fluorescence measurements. Analysis is non-destructive and, in the case of energy-dispersive X-ray analysis, many environmentally important elements can be measured simultaneously using a single calibration.

We describe the design and operation of an automated air-particulate analysis system based on energy-dispersive X-ray spectroscopy.[1] The instrument is capable of the unattended analysis of over 30 filter samples for up to 35 elements on each sample. A complete analysis cycle for each filter requires 30 min., although analysis for 15 environmental significant elements can be performed in only ten minutes. No sample preparation is required, only long term calibration checks are necessary, and the analysis results are immediately available.

Before describing the system and experimental results, we will present a brief discussion of the basic energy dispersive spectroscopy method and show how these are applied to the instrument design. More detailed accounts of X-ray fluorescence techniques are contained in the literature[2,3], as are accounts of the energy dispersive method.[4,5]

PHOTO-EXCITED ENERGY-DISPERSIVE X-RAY FLUORESCENCE

The X-ray fluorescence method is illustrated in Fig. 1. Incoming radiation interacts in the sample to produce vacancies within the inner shells of the atoms of interest; these vacancies then de-excite with the accompanying emission of fluorescent X-rays whose energies are characteristic of elements in the sample. The term "photon-excited" refers to the

character of the exciting radiation which, in the present case, consists of X-ray photons of sufficient energy to ionize the atomic shells in elements of interest. Alternative methods of excitation include electrons and positive ions. Although the latter has been proposed for a number of environmental monitoring purposes, its capabilities are in general inferior to that of photon-excitation with the exception of some rather specific sample forms.[6,7]

"Energy-dispersive" refers to the method of measurement of the X-ray energies to distinguish it from the more traditional wavelength-dispersive techniques.[2,3] In the energy-dispersive method, a semiconductor radiation detector measures the free charge produced in the ionization cascade following the photoelectric interaction of the X-ray within the active volume of the semiconductor crystal. This charge is proportional to the energy of the original X-ray. Resulting signals can be used as a measure of the energies of the incident X-rays over a wide energy range. This multiple-element analysis capability constitutes an important advantage of the energy-dispersive method in elemental contamination surveys, and in studies of the interaction of combinations of elements in pollution studies.

Figure 2 is a schematic of the X-ray spectrometer system including detector and processing electronics. The lithium-drifted silicon detector, normally 3 to 5 mm thick and 0.5 to 1 cm in diameter is cooled to liquid-nitrogen temperature, primarily to reduce its leakage current (resulting from thermally generated charge carriers) and the associated electrical noise to a very low value. Charge carriers (holes and electrons) result from the absorption of X-rays on the detector and are collected by applying an electric field across the active volume of the detector. The signal current through the detector is integrated by the first stage of the amplifier and the resulting step-function signals are amplified and shaped in a main amplifier unit before being fed to a pulse-height analyzer (or compuuter). The pulse height spectrum then represents a histogram of the number of events of various X-ray energies incident on the detector.

The energy resolution of the system determines its capability to resolve X-rays from adjacent elements in the periodic table, and also affects the detectable limit for analysis of elements in the presence of background.

The resolution is dependent both in the basic ionization process in the detector and on the signal/noise capabilities of the pulse processing electronics. Advances in the latter areas have made energy-dispersive X-ray analysis possible. Modern spectrometers are capable of energy resolutions more than adequate to resolve the characteristic K X-ray of those elements having atomic numbers greater than sodium. Analytical sensitivities in the <1 ppm range are routinely achieved for many elements, although the general question of detectability is complicated by the possible presence of overlapping lines from more than one element.

The pulse-height spectrum observed in fluorescence analysis contains peaks of the characteristic X-ray of interest together with a large number of events due to the scattering of the primary beam in the region of the sample. This scattering can occur either without energy loss by the primary photon (Rayleigh) or with a small energy loss depending on the scattering angle (Compton). Figure 3 is an idealized spectrum observed by irradiating a sample with monoenergetic primary photons. The two large peaks correspond to the scattering discussed above, the distribution at low energies is caused by scattering occuring in the detector itself. Fluorescent X-rays are evident in the middle of the spectrum superimposed on a low background due to numerous processes which can contribute to partial amplitude signals (e.g., multiple scattering, incomplete charge collection in the detector). A substantial reduction in background can be realized using a guard-ring detector with special pulse-rejection circuitry.[8] This unique system eliminates many of the causes of incomplete charge collection which can occur in the detector.

The use of monoenergetic excitation results in the lowest background level in the region of interest. This form of primary radiation can be approximated by the characteristic K_α and K_β X-ray spectrum of a selected target. In the present system, a target is irradiated with the primary radiation from a tungsten anode X-ray tube and the fluorescent X-rays from the target excite the sample. This "secondary fluorescence" geometry allows the exciting X-rays striking the sample to be varied in energy by changing the secondary fluorescence target. This technique

can be used to compensate for the dependence of excitation efficiency upon the difference between the energy of the characteristic X-ray and the primary radiation. Figure 4 shows plots of the relative probability of excitation of different elements for the three secondary targets selected for the present system. The excitation probability is calculated from fundamental properties of ionization cross sections and fluorescence yield and can be converted directly to analytical sensitivity in the case of energy-dispersive analysis. An important feature to note is the smooth variation of the X-ray production probability as a function of the Z of elements for each of the curves. This implies that a calibration curve can easily be interpolated between adjacent Z elements in cases where calibration standards cannot be conveniently prepared. Furthermore, the shape of these curves is not dependent on the X-ray tube-sample-detector geometry; a measurement on a single element standard corrects for the geometry factors and provides a sensitivity calibration for the whole range of elements covered by one fluorescer target.

INSTRUMENT DESIGN

Figure 5 is a cross section of the spectrometer illustrating the close-coupled X-ray tube/secondary target/sample geometry. With these large solid angles we are able to operate at maximum counting rates of 10,000 counts/sec using less than 40 watts of anode power in the X-ray tube. The secondary targets can be automatically switched to provide a variable energy of fluorescence excitation; the present targets are Cu, Mo, and Tb. Over 30 air filters mounted in special holders can be sequenced through a complete analysis cycle without operator intervention.

Control and monitoring functions together with data acquisition and analysis are carried out by a small on-line computer. The secondary target sequence and the dead-time corrected counting interval are chosen via front panel switches. Upon pressing a "start" button, the system will automatically perform the desired analysis and print out the results in ng/cm^2 for each of the filters in the stack loader. In addition to the printed output, the system also writes the original spectral data and the results of the data reduction on magnetic tape.

Figures 6 and 7 are logarithmic plots of X-ray fluorescence spectra acquired on the same air filter in five minute counting intervals using the Mo and Cu fluorescence respectively. Typical concentrations for some of the observed elements are PB-1.32 $\mu g/cm^2$, Fe-0.5 $\mu g/cm^2$, Mn-30 ng/cm^2 and Ca-0.5 $\mu g/cm^2$. The spectral response is similar to that shown in Fig. 3 with appropriate adjustment for the presence of both a K_α and K_β peak in the spectrum of exciting radiation. The improved peak to background for light elements is apparent in the spectrum acquired using the Ca excitation.

DATA ANALYSIS

The multiple-element capability of the energy dispersive method is illustrated in the large number of peaks in the spectra. For the method to be quantitative, the areas of individual peaks must be extracted from the data and an appropriate calibration applied. The principal problems associated with performing this computer analysis are subtraction of the continuous background from the region of interest and correction for interference between peaks of different elements due to the multiple structure of X-ray spectra. Both problems are solved by using a large memory in the computer to store spectra derived from a blank filter and from elements of interest. Experience shows that the background is relatively insensitive to the impruity concentration on a filter, so a blank filter can be run to provide a background spectrum that includes any impurity element either in the filter material or arising from the system itself.

Figure 8 shows a schematic sequence of the operations in the program. The original spectrum is sequentially reduced by first subtracting an appropriate multiple of the stored background compared over a selected region, and then by sequentially stripping out each of the spectra due to the individual elements. The factor which determines the amount of each elemental spectrum to be subtracted, which is determined by the computer, is simply related to the area of the peak. Peak areas are then converted to concentrations in ng/cm^2 by applying the appropriate excitation and detection efficiency function similar to those shown in Fig. 4.

CALIBRATION

The expression given in Fig. 9 is the formal mathematical expression of the intensity of the K X-ray for element i for the case of monoenergetic photons of energy E_o and intensity I_o incident on a slab of thickness d. The quantity $p_i d$ is the mass in ng/cm^2; other parameters are G, the solid angle, τ_i the photoelectric cross section for element i for photons of energy E_o, w_k^i the fluorescence yield for the K or L shell vacancies, ε_i the efficiency for detecting the fluorescent X-rays, and μ_o and μ_i are the total mass absorption coefficients for the incident and fluorescent radiations respectively. The quantity in brackets is, in effect, a correction for the absorption experienced by the radiation for thick samples. In most air filter applications it can be neglected except for very light element analyses (Z = 20).

The equation can, in principle, relate the area of the peak (I_i) to the concentration ($p_i d$) if the physical parameters are either measured or taken from literature values. In practice it proves more reliable to measure the complete function for a few selected elements and interpolate a smooth curve between the data for the remaining elements. Figure 10 is a plot of a family of curves obtained using a series of thin-film evaporated standards. The results can be compared directly with the purely theoretical results shown in Fig. 4. The discrepancy for heavier elements is due to the rapid decrease in detector efficiency at higher X-ray energies which was not included in the calculations. Since the shape of these curves is invariant for a fixed fluorescence-sample-detector geometry, subsequent calibrations only involve renormalization for variations in intensity of the exciting radiation, and can be achieved by measuring a single-element standard. Experience has shown that the stability of the system is sufficient to obviate the need for frequent calibrations.

Using the above curves, the validation results given in Table 1 were achieved. The majority of standard samples were in the form of thin evaporated films although a number of elements were checked using compounds with

known elemental ratios. These measurements were independent of any prior calibration data. The results include the automatic computer analysis. The agreement represents an average deviation of less than 5% over all elements.

RESULTS

The performance of any analytical system is judged from the demonstrated accuracy which it can achieve with realistic samples--in our case air filters. Table 2 is a comparison of the results obtained in the automatic analysis of a series of eight air filter samples taken on Millipore backings. The results marked (i) are the present measurements, whereas (ii) represent value obtained by carefully executed manual X-ray fluorescence measurements by R. Giauque in our laboratory. His system and method have been extensively checked and validated by alternative analytical methods.[4] The agreement between the two sets of measurements is within the quoted errors in most cases; a significant achievement when one considers that the present analyses were performed in less than one hour without operator intervention.

A series of separate validation results have been obtained for a number of elements using neutron activation as a comparison. General agreement between the two methods has been within 10%.[9]

The sensitivity of the technique for detection of elements present in very small quantities has been evaluated by measuring the minimum detectable limit for the various elements. This is defined as the quantity of material required to give a peak area equal to three times the statistical error in the background under the peak during a five minute counting interval. These measurements also include the filter flow rate of our associated air samples which was measured to be 0.8 m^3 of air/cm^2 of filter material over the two hour sampling period. The minimum detectable levels shown in Fig. 11 are quoted in ng/m^3 of air for the above samples. To convert to ng/cm^2 on the Millipore filter, the results should be multiplied by 0.8. To a first approximation these detection curves should correlate with the relative efficiency factors shown in Fig. 10. Slight difference in the shape of the curves results from variations in the shape of the background

for a given fluorescer; relative differences from one fluorescer to the next are also affected by the difference in the incident X-ray yield for each X-ray tube setting. In particular, this largely accounts for the values for detectability measured for Tb excitation being worse than would be expected on the basis of the calculated sensitivities.

An important consideration in comparing these detectable limits with results obtained for competing methods is the multiple-element detection capability of energy-dispersive X-ray fluorescence. The three curve segments in Fig. 11 represents the sensitivities for simultaneous detection of many elements excited with each of the three fluorescers. (This statement is not rigorously accurate since it neglects reduction in detectability due to interelement interferences; however, in cases where the variation in concentration between adjacent elements is not large, the data are accurate enough for comparison.) It can be argued that the sensitivity could be optimized for one element, by filtering the X-rays. However, one of the greatest strengths of the energy-dispersive method is its multi-element capability which would appear to be important in environmental research and monitoring. Any comparison of the cost of analysis with that of competing analytical methods should bear this in mind.

PARTICLE SIZE AND MATRIX EFFECTS

As noted earlier, calibration problems arise for light elements due to the absorption of the low-energy characteristic X-rays either by the filter matrix or by the individual aerosol particles. Since the mean absorption length for these X-rays may be short compared to particle diameters, or to the filter thickness, the X-ray intensity reaching the detector depends upon the microscopic location from which the X-ray is generated either within the particle or in the filter matrix. Calculations of elemental concentrations using the observed X-ray intensity must then include a correction for this effect.

To calculate a reasonable correction factor, it is necessary to know something about the particle size distribution and the location of the intercepted particles within the filter material. Information concerning particle size must be obtained either by restricting the size range reaching the filter (e.g., using impactors), or by making some assumptions regarding the size distribution in the original aerosols. Similarily, the absorption correction due to the filter matrix must be estimated by assuming localization of the particles in the filter, most likely on its surface.

At its best, any assumption appears to have dubious merit, so we have limited our investigation of the problem to estimating the maximum effect anticipated in certain limiting cases. This has been done by calculating the difference between the observed X-ray intensity with and without the absorption effects. Referring to Fig. 9 we see that the difference between a thin film X-ray intensity and that including the absorption of the X-rays integrated over a thickness d is given by a factor

$$A = \frac{1 - e^{-(\mu_0 + \mu_1)\, \rho d}}{(\mu_0 + \mu_1)\, \rho\, d} \qquad (1)$$

where μ_0 and μ_1 are the total absorption coefficient for the exciting and emitted radiation respectively. If we now associate d with the diameter of a homogeneous particle, we can calculate the absorption correction A as a function of particle size. (This calculation will overestimate the correction for spherical particles since it assumes a constant thickness; however, since so little is known about particle shapes, the assumption is as valid as any other.) Figures 12, 13 and 14 are the results of calculations for the case of Al, S and Ca X-rays excited by Cu Kα radiation. The individual curves represent various assumptions regarding particle composition; the hydrocarbon assumes a unit density material having the absorption cross sections of carbon. The results indicate that no serious problems

occur for particles of size below 10 μ except in the case of Al. Estimates of matrix effects can also be obtained from these curves by recognizing that the 5 ng/cm^2 Millipore filter is equivalent to a 50 μ thick hydrocarbon sample. Thus, if the material were uniformly distributed throughout the filter, the correction to the intensity at its maximum would be the value of the hydrocarbon absorption correction at 50 μ. Again the correction is not too serious except in the case of Al.

These families of curves represent a guess as to likely chemical constituents of particles. It is possible that more difficult combinations of elements might produce significant absorption effects (PbS is an obvious candidate). Again we are faced with the necessity of making some assumptions regarding the nature of particulates in order to estimate the correction factor.

The problems associated with these effects are of course inherent to the X-ray fluorescence method and are the same regardless of how one excites or detects the radiation. However, additional information can be obtained by using a monoenergetic X-ray source to excite the characteristic radiation. As noted in Eq. 1, the correction factor depends upon the absorption coefficient for both the incident and emitted X-rays. By varying the incident X-ray energy, two measurements can be performed, one in which absorption of the incident radiation is neglible over the particle diameter, and the other where it is significant. Another way of looking at the problem is to consider the higher energy excitation as a probe measuring the total particle volume, whereas the low-energy excitation samples the surface only. In this way information regarding the absorption characteristics of the particle can be obtained. To a first approximation, this measured absorption correction would be independent of any assumptions regarding particle shape or composition. A similar arguement could be applied to the question of matrix absorption within the filter.

SUMMARY AND CONCLUSIONS

The successful application of recently developed energy dispersive X-ray analysis techniques to the automated elemental analysis of atmospheric aerosol particulates has been demonstrated. Detectabilities for a number of environmental important elements have been shown to be within practical limit for research and monitoring purposes. Although the emphasis of the design has been toward optimum results for air filter samples, the basic ideas can also be applied to the multi-element analysis of a large class of samples.[10] Future improvements in the system performance may be realized by the incorporation of high-rate pulse excitation,[11] and polarization scattering geometries.[12] Current work is being devoted to those and other innovations which might improve the calibration of the system.

ACKNOWLEDGEMENT

We wish to acknowledge the important contributions to the design of the system which were made by D. Landis and B. Loo. We also acknowledge the efforts of F. Gin, A. Jue, W. Searles, G. Skipper and S. Wright in the fabrication and testing of the equipment; J. Walton and H. Sommer in detector fabrication, and J. Anderson and D. Malone in the construction of mechanical assemblies. We have profited from discussions and consultations with many people including T. Dzubay, R. Hammerle and R. Giauque. Further appreciation is expressed to R. Giauque for his continuing copperation in the analysis of samples for comparison purposes.

REFERENCES

1. Goulding, F. S. and Jaklevic, J. M. "X-Ray Fluorescence Spectrometer for Airborne Particulate Monitoring" Final Report to the Environmental Protection Agency, EPA Report No. EPA-R2-73-182 (1973).

2. Liebhafsky, H. A., Pfeiffer, H. G., Winslow, E. H. and Zemany, P. D. X-ray Absorption and Emission in Analytical Chemistry (New York: John Wiley and Sons, 1960).

3. Birks, L. S. X-ray Spectrochemical Analysis (New York: Interscience Publishers, John Wiley and Sons, 1969).

4. Giauque, R. D., Goulding F. S., Jaklevic, J. M. and Pehl, R. H., "Trace Element Determination with Semiconductor Detector X-ray Spectrometers" Anal. Chem. 45, 671 (1973).

5. Russ, J. C. Energy Dispersion X-Ray Analysis: X-Ray and Electron Probe Analysis (Philadelphia: American Society for Testing and Materials, ASTM Publ. 485, 1970).

6. Cooper, J. A., Nucl. Instrum. and Methods 106, 525-538 (1973).

7. Cahill, T. A. "Cyclotron Analysis of Atmospheric Contaminents" Final Report to the California Air Resources Board, Crocker Nuclear Lab Report No. UCD-CNL-162 (1972).

8. Goulding, F. S., Jaklevic, J. M., Jarrett, B. V. and Landis, D. A. "Detector Background and Sensitivity of X-ray Fluorescence Spectrometers" Advances in X-ray Analysis, 15, 470-482 (New York: Plenum Press 1972).

9. Hammerle, R. H., Marsh, R. H., Rengan, K., Giauque, R. D. and Jaklevic, J. M., "A Test of X-ray Fluorescence as a Method for Analysis of the Elemental Composition of Atmospheric Aerosol". To be published in Annalytical Chemistry.

10. Jaklevic, J. M. and Goulding, F. S. "Semiconductor Detector X-ray Fluorescence Spectrometry Applied to Environmental and Biological Analysis", IEEE Trans. Nucl. Sci. NS-19, #3, 384-391 (1972).

11. Jaklevic, J. M., Goulding, F. S. and Landis, D. A. "High Rate X-ray Fluorescence Analysis by Pulsed Excitation", IEEE Trans. Nucl. Sci. NS-19, #3, 392-395 (1972).

12. Dzubay, T. G., Jarrett, B. V. and Jaklevic, J. M., "Background Reduction in X-ray Fluorescence Spectra Using Polarization". To be published in Nuclear Instruments and Methods.

Table 1. Comparison of Measured Concentration of Standard Samples

ELEMENT	FLUORESCER	MEASURED DENSITY[a] ($\mu g/cm^2$)	ACCEPTED VALUE[b] ($\mu g/cm^2$)
Al	Cu	1550 c)	2200 d)
Si	Cu	2380	2430 d)
S	Cu	2820	2970 d)
Ti	Cu	90	101
Cr	Cu	117	122
Fe	Cu	83 e)	83
Ti	Mo	100	101
Cr	Mo	121	120
Fe	Mo	94	87
Ni	Mo	109	100
Cu	Mo	55	49
Pb	Mo	132	131
Zr	Tb	66	61 f)
Pd	Tb	138	142
Cd	Tb	92	93 f)
Sn	Tb	142	138
Ba	Tb	122	124 f)

a) Statistical errors are less than 1% in all cases of evaporated films.

b) Thicknesses of evaporated films were determined by weighing. Estimated errors are <5%.

c) The discrepancy in this comparison could easily be due to heavy elements in the 1100 Al alloy used.

d) These densities represent the effective weight of infinitely thick samples.

e) The Cu fluorescer comparisons are normalized to the Fe value.

f) These were obtained by using samples of $ZrBr_4$, $CdBr_2$, and $BaBr_2$; the Br intensity was measured with the Mo fluorescer.

Table 2. Comparison of Results Obtained on Several Filter Samples

		SAMPLE NUMBER 1	2	3	4	5	6	7	8
Ca	(i)	261 ±17	328 ±18	333 ±18	343 ±18	298 ±18	236 ±17	199 ±16	435 ±20
	(ii)	271 ±25	393 ±25	361 ±25	383 ±44	286 ±45	200 ±43	177 ±42	523 ±52
Ti	(i)	30 ± 7	43 ±12	35 ±10	38 ±12	27 ± 9	16 ± 6	19 ± 6	41 ±12
	(ii)	37 ±18	47 ±20	48 ±10	49 ±20	42 ±15	62 ±20	43 ±15	66 ±15
Mn	(i)	<5	7 ± 5	2 ± 5	26 ± 5	8 ± 5	<5	<5	22 ± 5
	(ii)	11 ± 4	6 ± 4	15 ± 4	27 ± 8	<23	<22	<22	27 ± 8
Fe	(i)	410 ± 8	463 ± 8	421 ± 8	575 ± 8	319 ± 7	212 ± 6	180 ± 6	501 ± 8
	(ii)	405 ±20	466 ±23	421 ±21	572 ±23	371 ±15	243 ±10	180 ± 9	480 ±19
Ni	(i)	8 ± 3	5 ± 3	<3	<3	<3	<3	<3	8 ± 3
	(ii)	4 ± 2	8 ± 2	<6	<11	<11	<11	<11	9 ± 4
Cu	(i)	97 ± 4	74 ± 4	83 ± 4	26 ± 3	4 ± 3	<3	<3	12 ± 3
	(ii)	81 ± 4	53 ± 3	55 ± 3	27 ± 4	7 ± 4	6 ± 4	6 ± 4	18 ± 4
Zn	(i)	59 ± 3	52 ± 3	43 ± 3	111 ± 3	23 ± 3	13 ± 3	10 ± 3	46 ± 3
	(ii)	58 ± 3	51 ± 3	41 ± 2	91 ± 4	24 ± 3	13 ± 3	12 ± 3	40 ± 3
Br	(i)	81 ± 3	157 ± 3	111 ± 3	170 ± 3	174 ± 3	129 ± 3	47 ± 3	394 ± 4
	(ii)	95 ± 5	175 ± 9	127 ± 5	171 ± 7	179 ± 7	129 ± 5	40 ± 4	408 ±16
Pb	(i)	354 ± 8	680 ± 8	451 ± 8	763 ± 9	665 ± 8	511 ± 8	198 ± 6	1329 ±11
	(ii)	327 ±16	716 ±36	449 ±22	747 ±30	702 ±28	563 ±23	196 ± 8	1320 ±53

a) Errors reflect counting statistics only. In case where the quoted error is less than 10%, a 10% calibration error should be assumed.

i) Values measured on EPA system.

ii) Values measured by R. Giauque.

FIGURE CAPTIONS

Fig. 1. Illustration of the principles of an X-ray fluorescence analyzer.

Fig. 2. The overall detector-electronics system used in an X-ray fluorescence analyzer.

Fig. 3. Idealized spectrum observed with an X-ray fluorescence analyzer.

Fig. 4. Calculated relative K X-ray production yields for three excitation energies (Cu Kα, Mo Kα, Tb Kα X-rays).

Fig. 5. Diagram of the geometry used in the final design.

Fig. 6. Air filters spectrum taken using the molybdenum fluorescer.

Fig. 7. Air filters spectrum taken using the copper fluorescer.

Fig. 8. Illustration of spectrum stripping procedure.

Fig. 9. Expression for the overall efficiency of the process of production, absorption and detection of the fluorescent X-rays.

Fig. 10. Actual relative efficiency curves for three fluorescers. These can be compared with the theoretical curves of Fig. 4.

Fig. 11. Elemental detection sensitivity curves for the three fluorescers (two hour sample collection time, five minute analysis time on each fluorescer).

Fig. 12. Calcium X-ray attenuation vs. particle size.

Fig. 13. Sulphur X-ray attenuation vs. particle size.

Fig. 14. Aluminum X-ray attenuation vs. particle size.

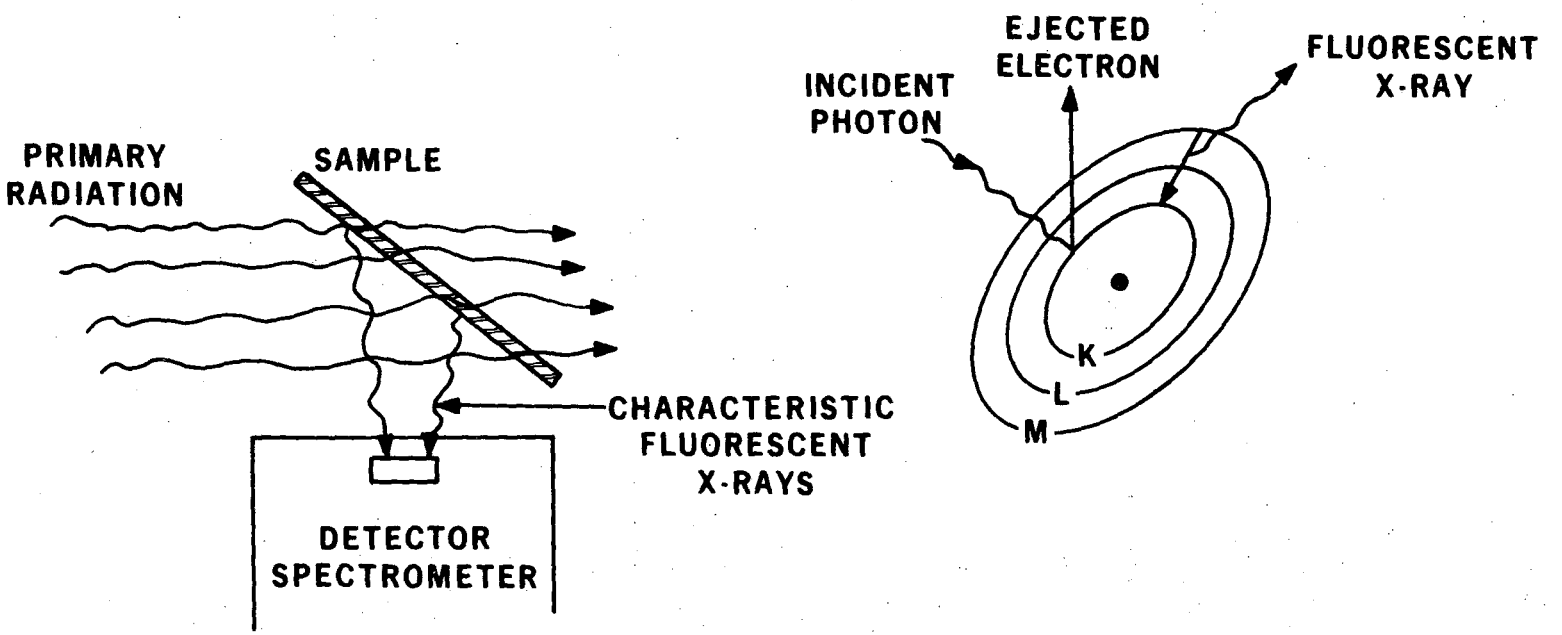

XBL 733-287

FIG. 1

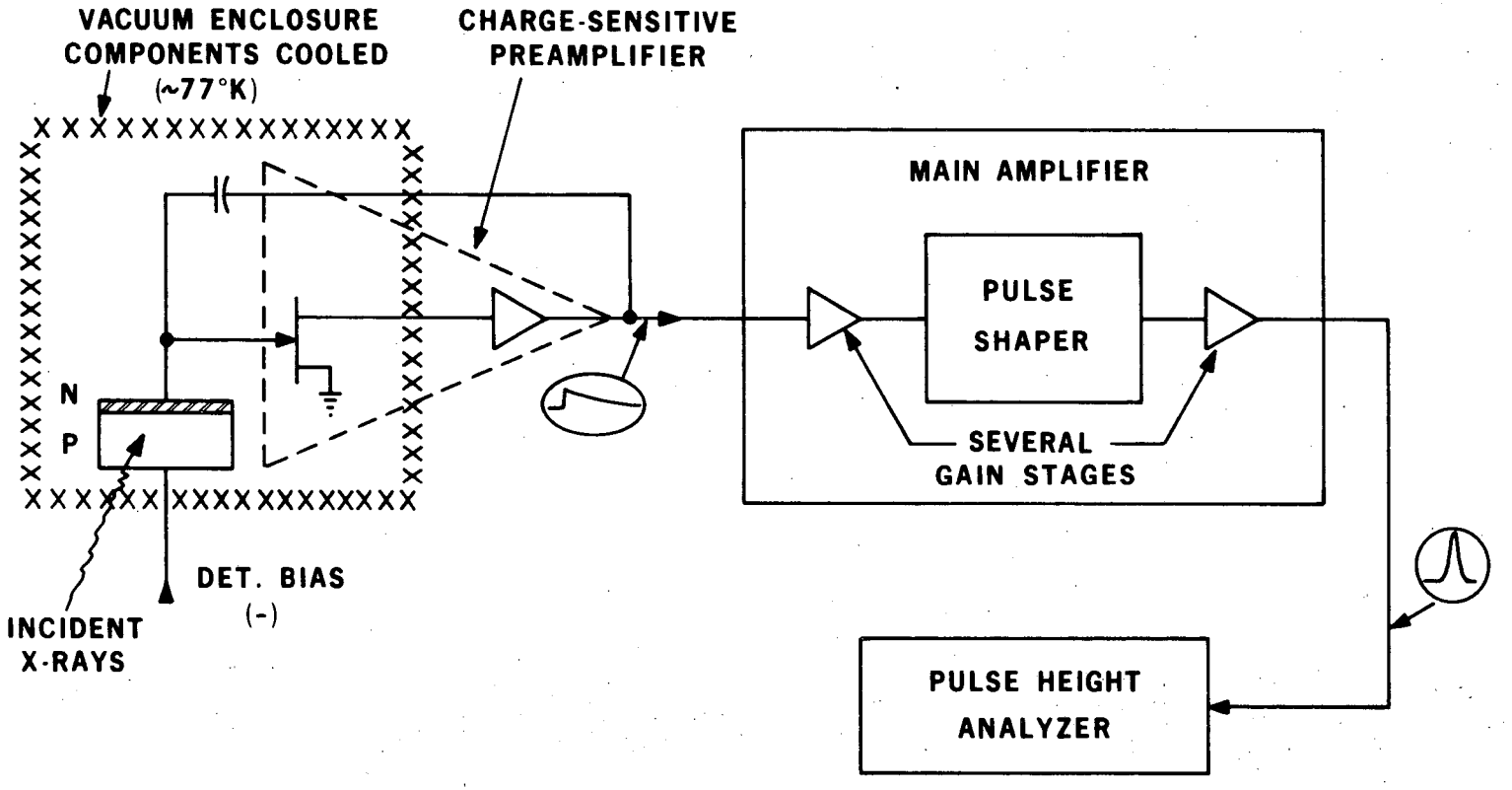
VACUUM ENCLOSURE
COMPONENTS COOLED
(~77°K)
CHARGE-SENSITIVE
PREAMPLIFIER
MAIN AMPLIFIER
PULSE
SHAPER
SEVERAL
GAIN STAGES
N
P
DET. BIAS
(-)
INCIDENT
X-RAYS
PULSE HEIGHT
ANALYZER
XBL 733-284

FIG. 2

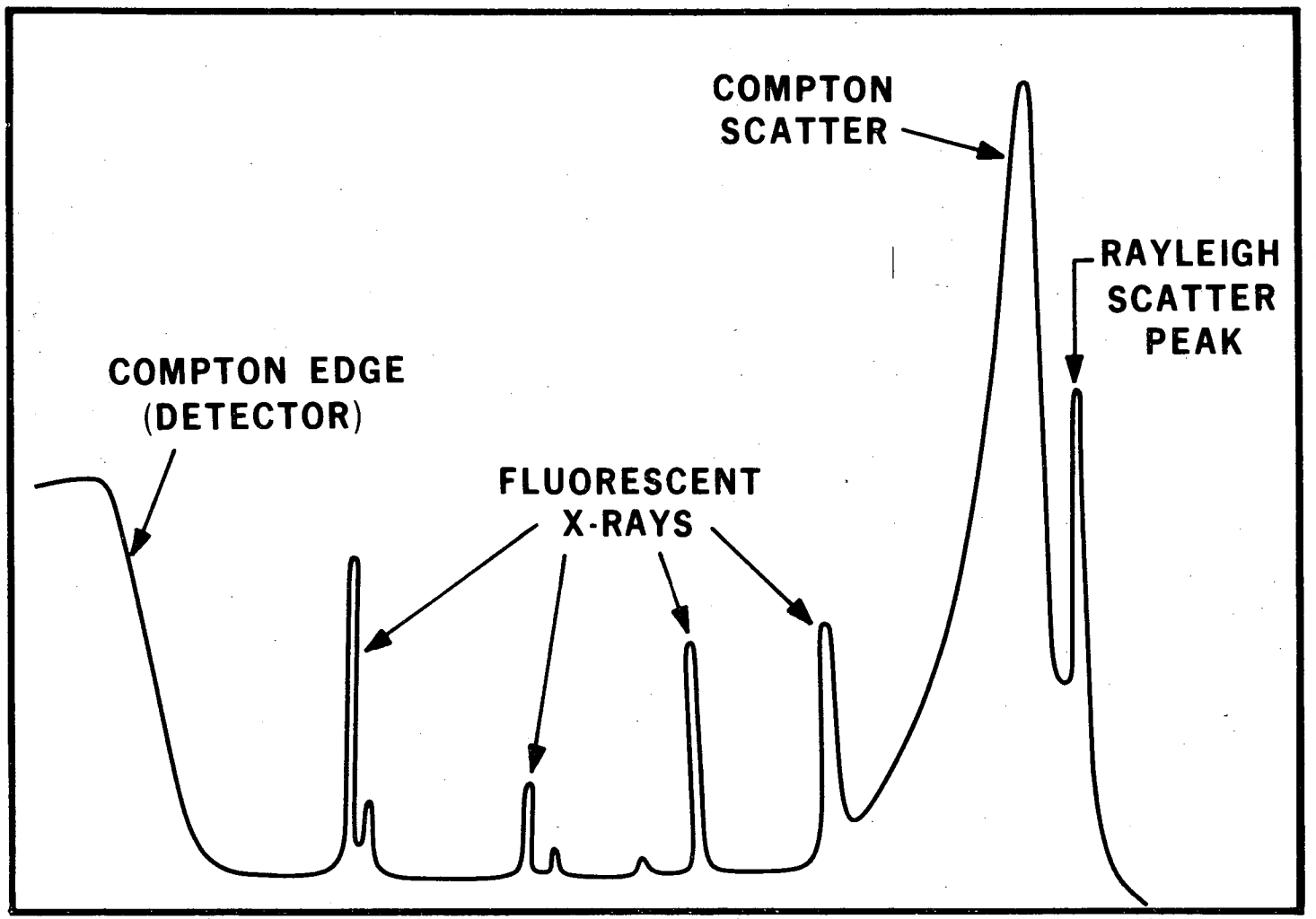

XBL 733-292

FIG. 3

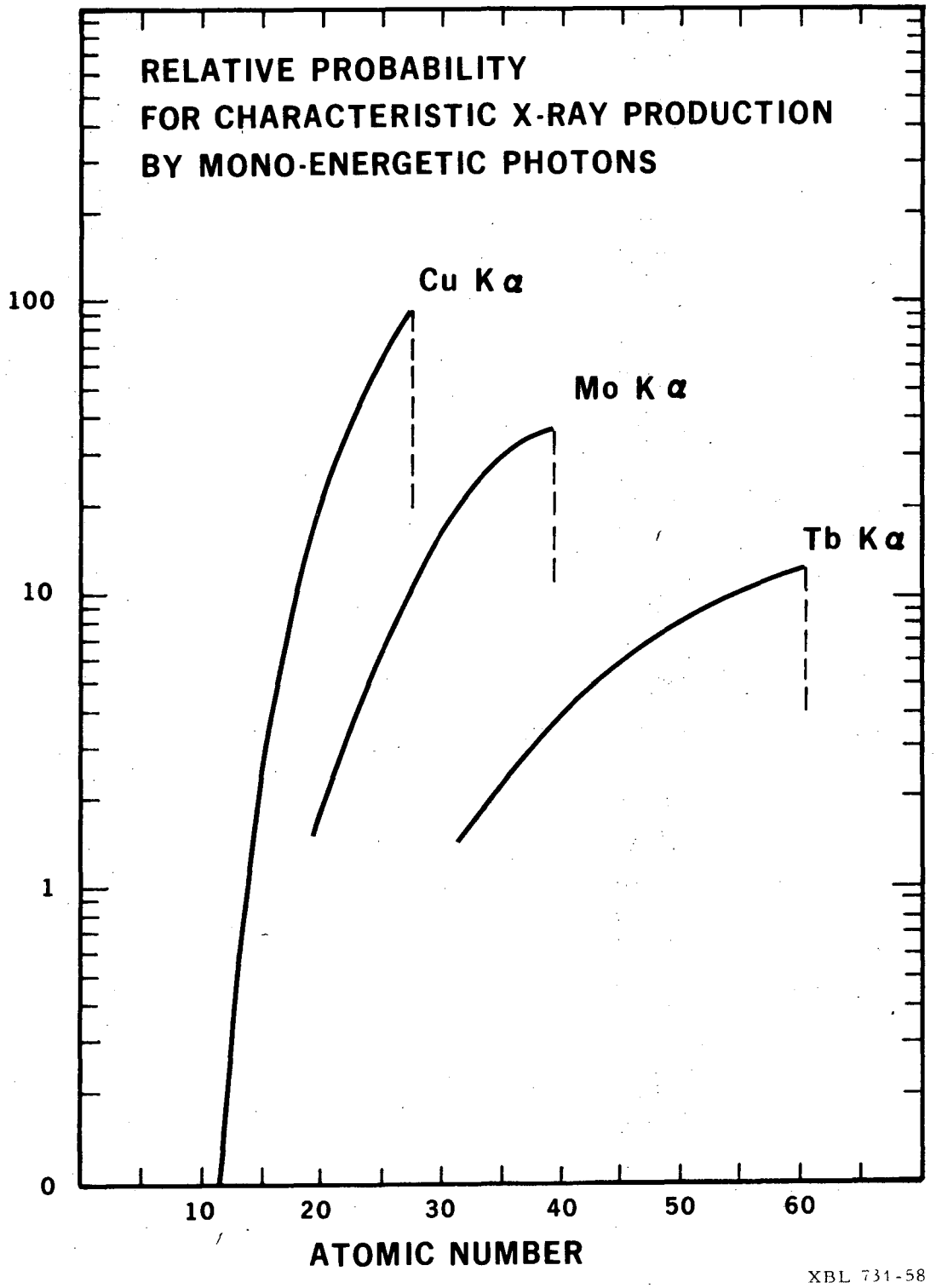
RELATIVE PROBABILITY
FOR CHARACTERISTIC X-RAY PRODUCTION
BY MONO-ENERGETIC PHOTONS
Cu Kα
Mo Kα
Tb Kα
100
10
1
0
10
20
30
40
50
60
ATOMIC NUMBER
XBL 731-58

FIG. 4

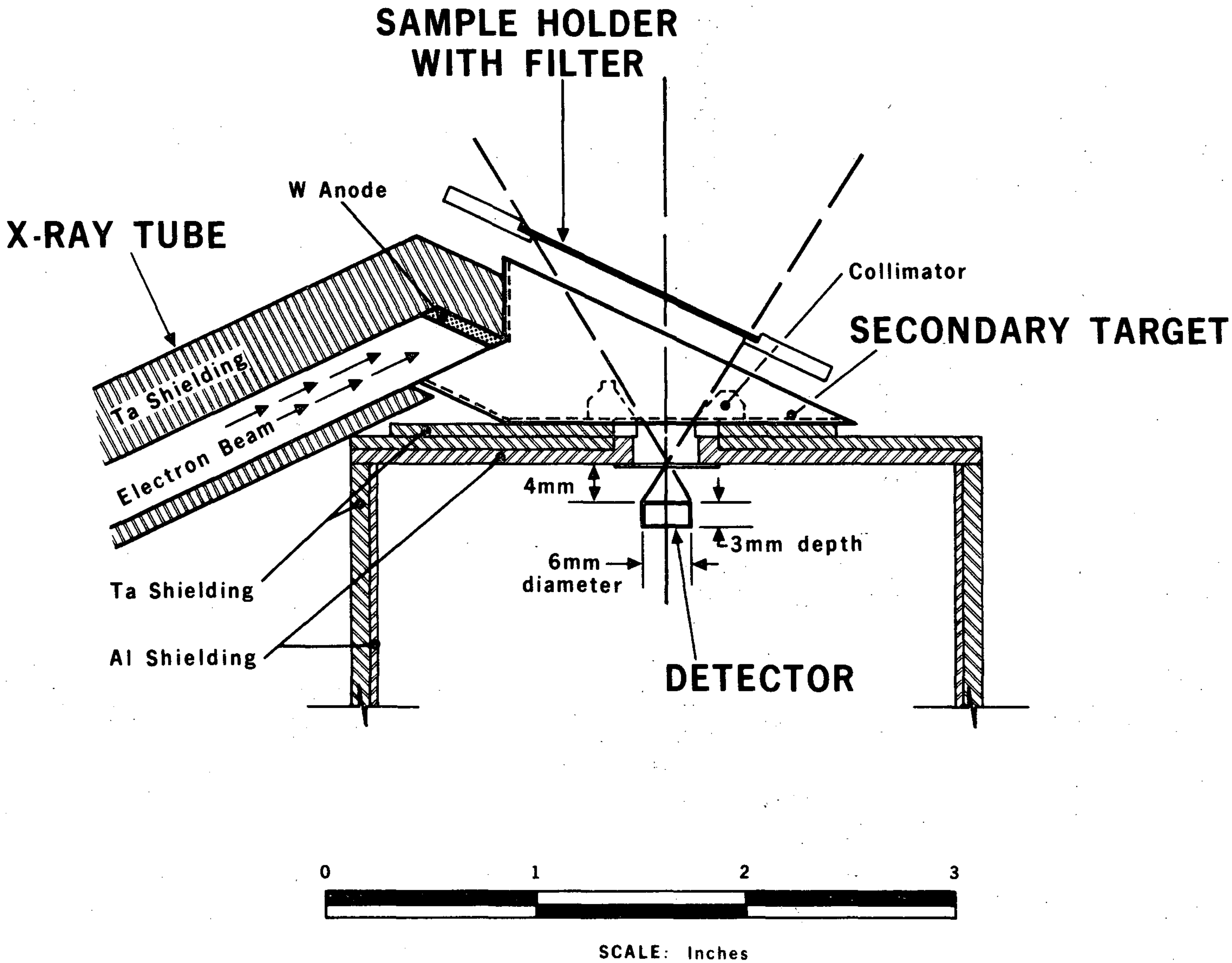

XBL 731-102

FIG. 5

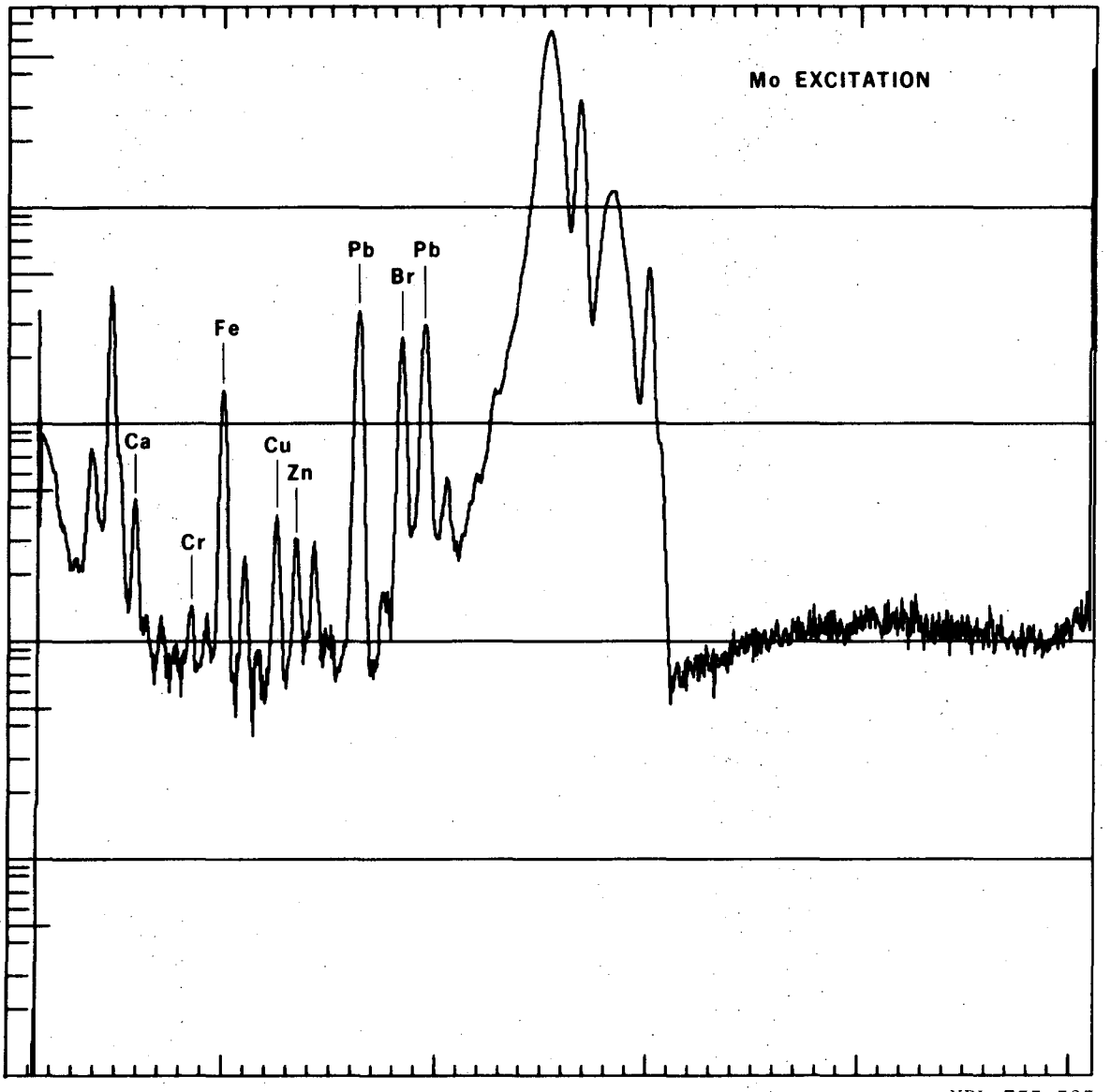

FIG. 6

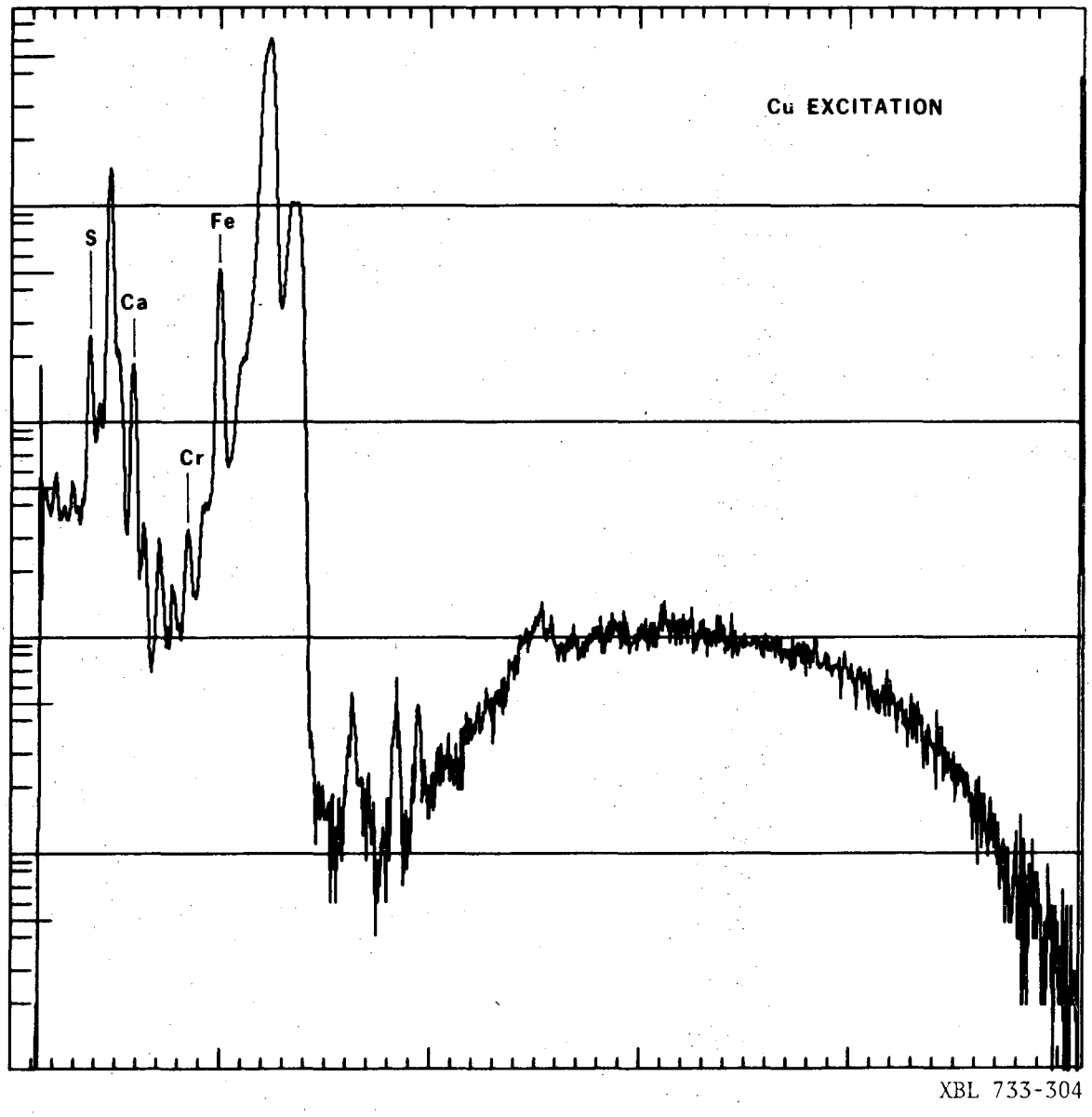

FIG. 7

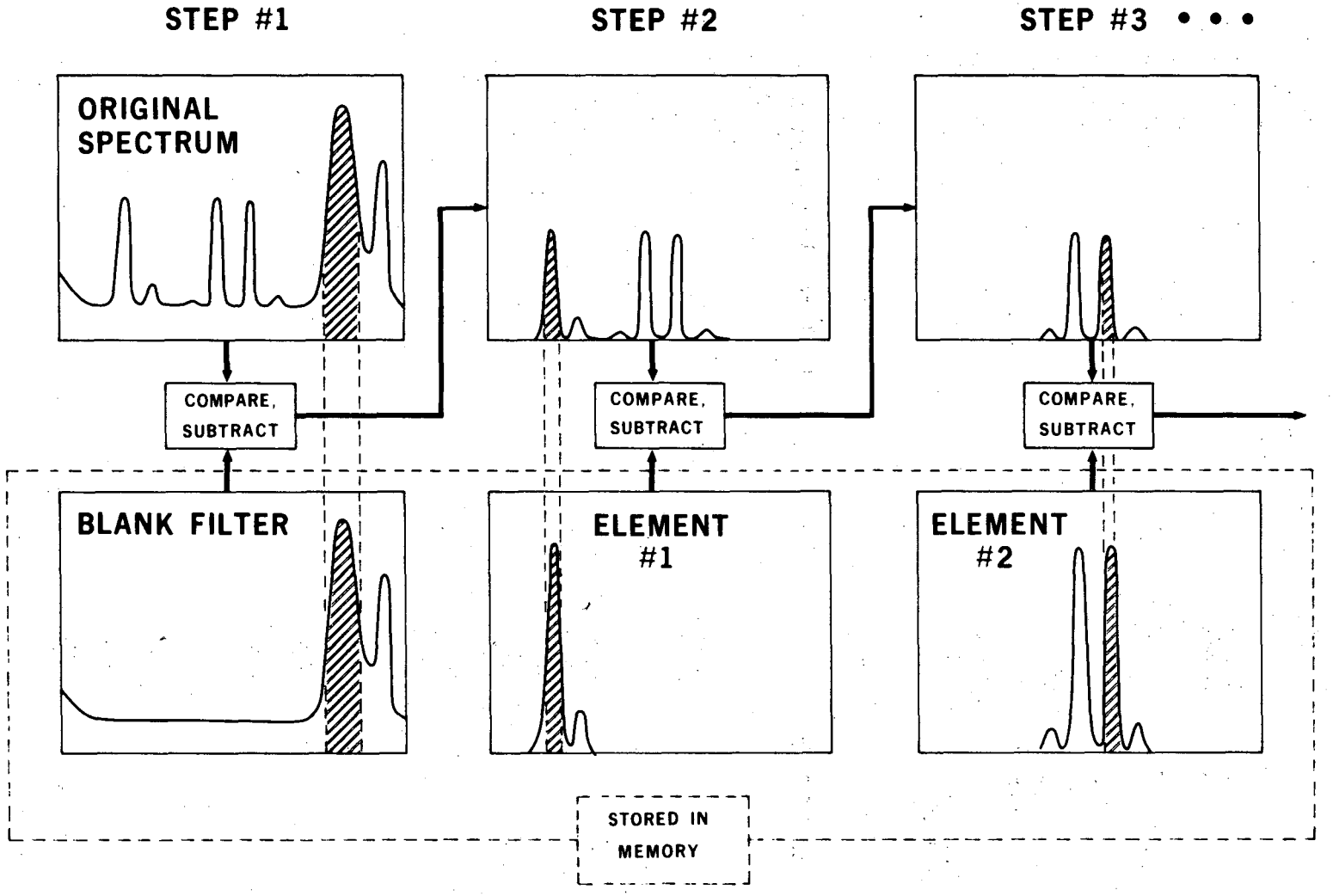
STEP #1
STEP #2
STEP #3 • • •
ORIGINAL SPECTRUM
COMPARE, SUBTRACT
COMPARE, SUBTRACT
COMPARE, SUBTRACT
BLANK FILTER
ELEMENT #1
ELEMENT #2
STORED IN MEMORY
XBL 731-86

FIG. 8

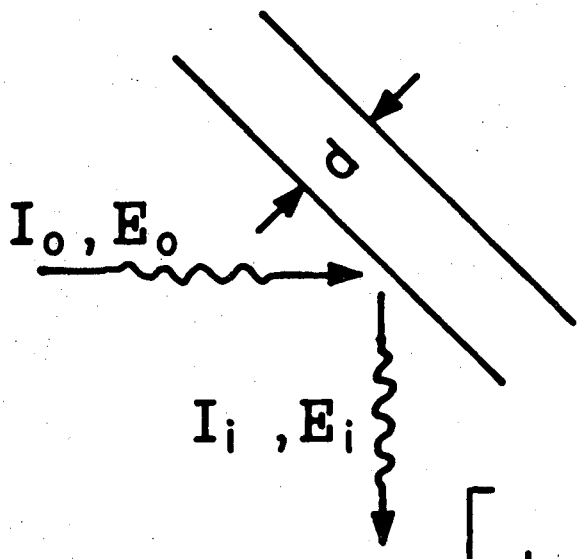

$$I_i = I_o G \rho_i d \tau_i \omega_k^i \epsilon_i \left[\frac{1 - e^{-(\mu_o + \mu_i)\rho d}}{(\mu_o + \mu_i)\rho d} \right]$$

XBL 7110-1500

FIG. 9

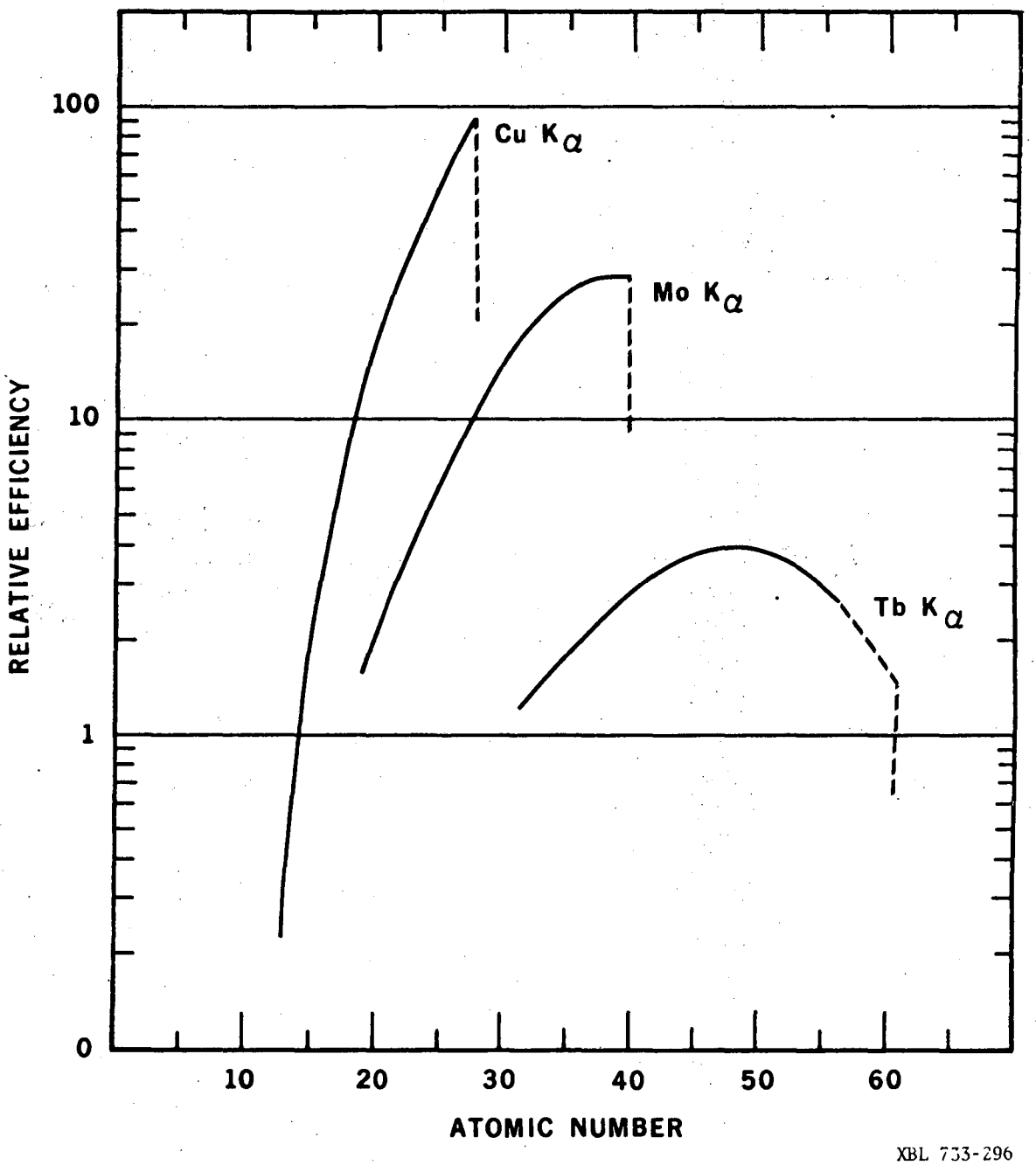
100
10
1
0
RELATIVE EFFICIENCY
Cu Kα
Mo Kα
Tb Kα
10
20
30
40
50
60
ATOMIC NUMBER
XBL 733-296

FIG. 10

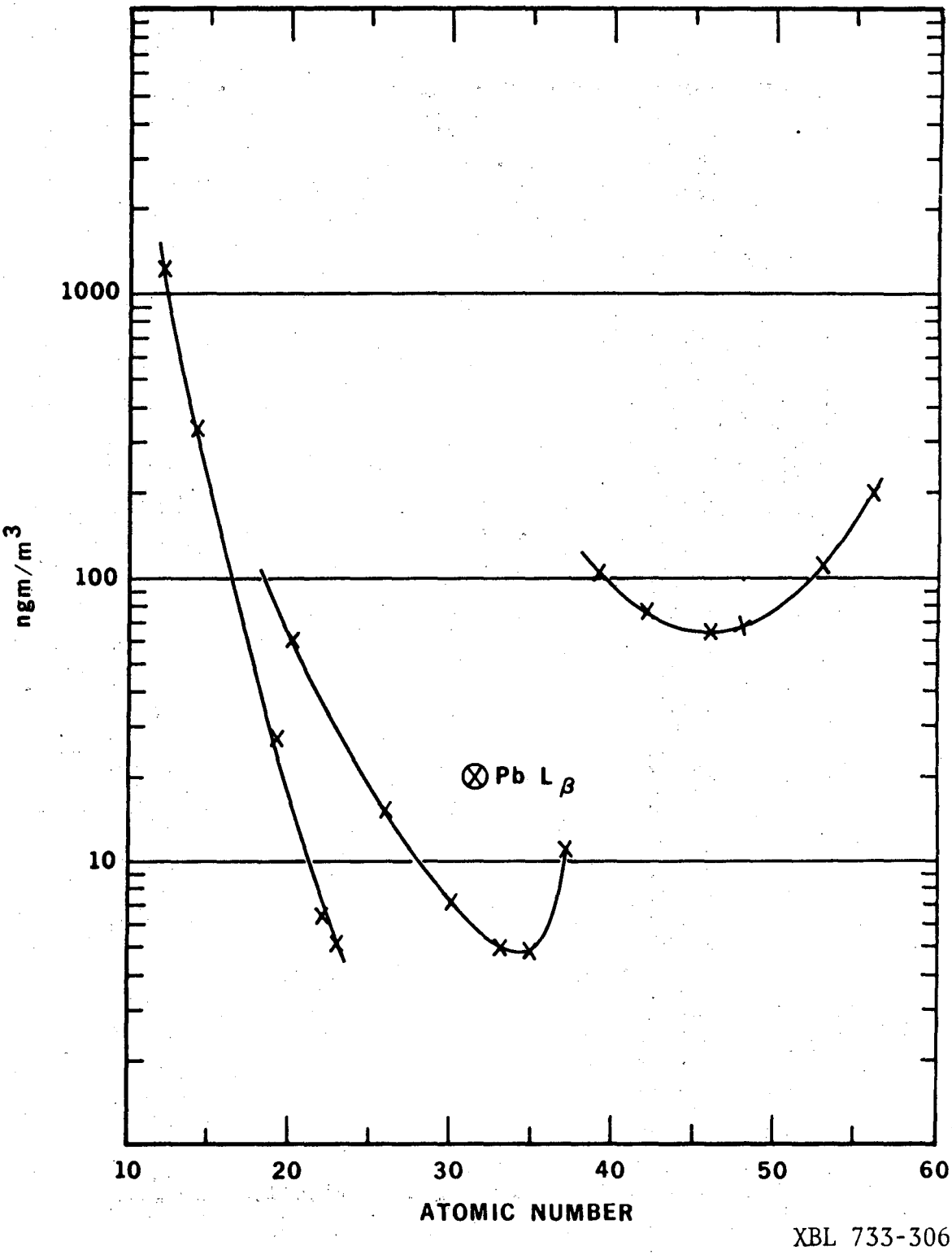
1000
100
10
ngm/m3
⊗Pb Lβ
10
20
30
40
50
60
ATOMIC NUMBER
XBL 733-306

FIG. 11

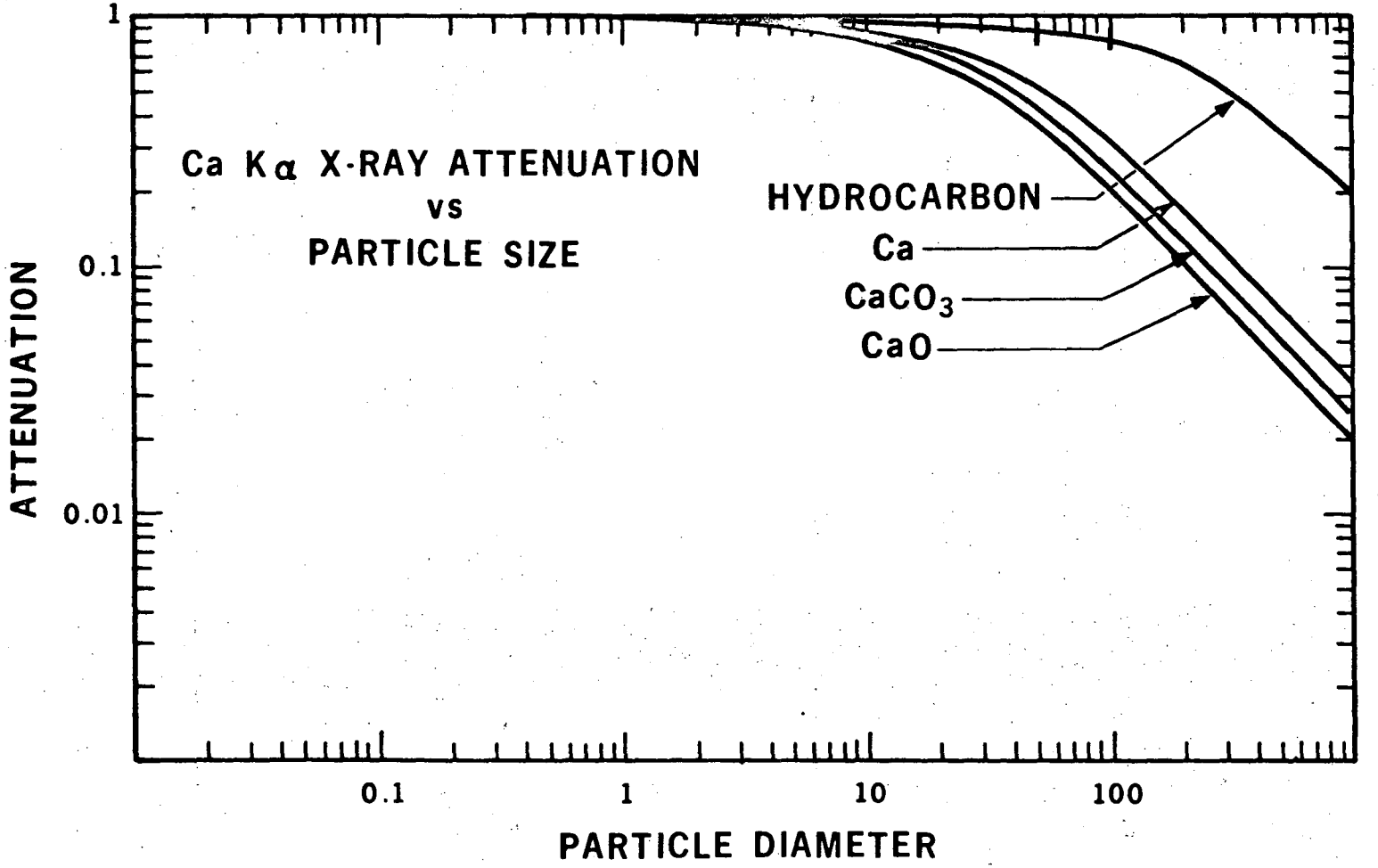
Ca Kα X-RAY ATTENUATION
vs
PARTICLE SIZE
HYDROCARBON
Ca
CaCO3
CaO
ATTENUATION
1
0.1
0.01
0.1
1
10
100
PARTICLE DIAMETER
XBL 731-60

FIG. 12

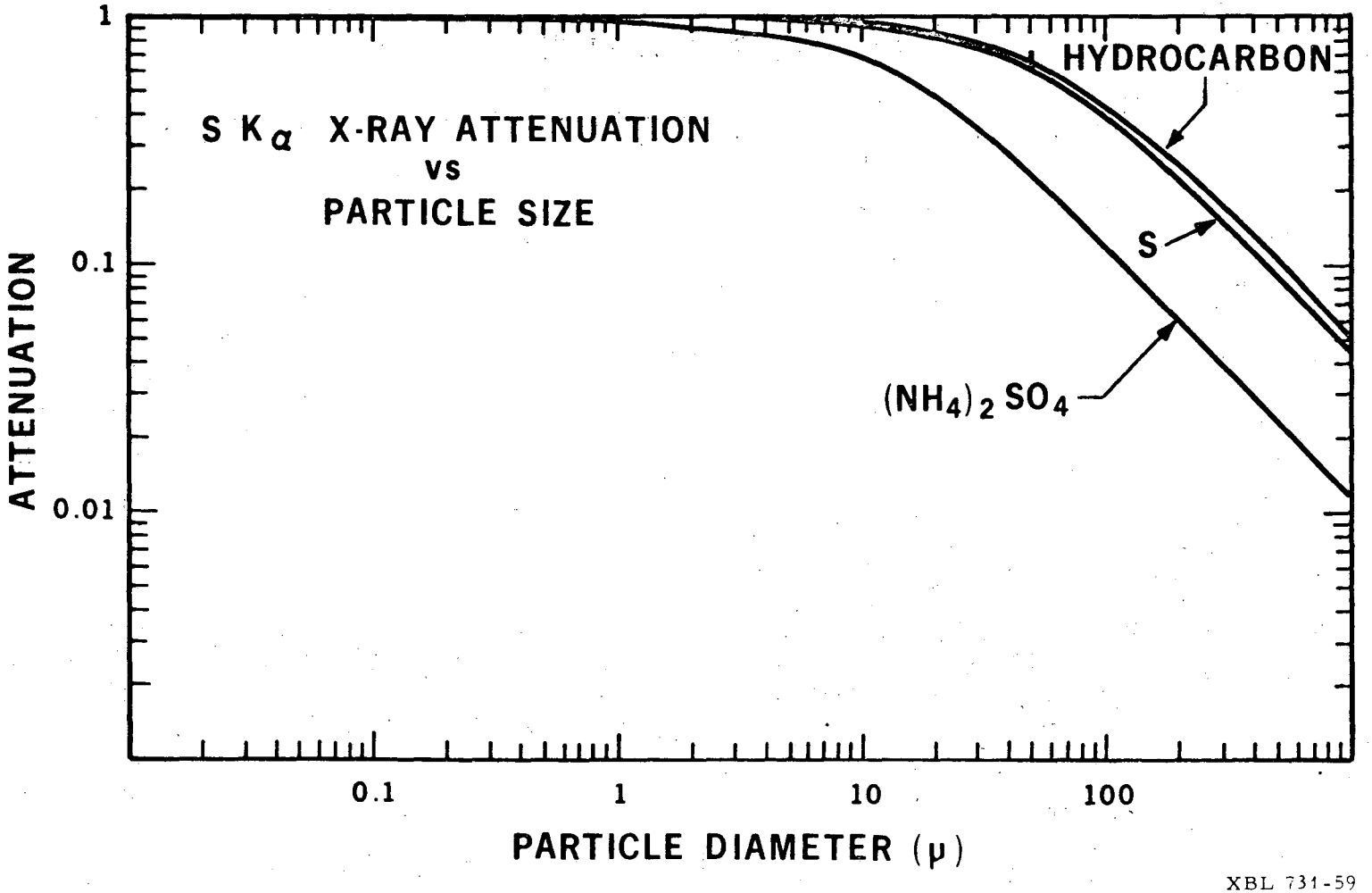
S Kα X-RAY ATTENUATION
vs
PARTICLE SIZE
HYDROCARBON
S
(NH4)2 SO4
ATTENUATION
1
0.1
0.01
0.1
1
10
100
PARTICLE DIAMETER (μ)
XBL 731-59

FIG. 13

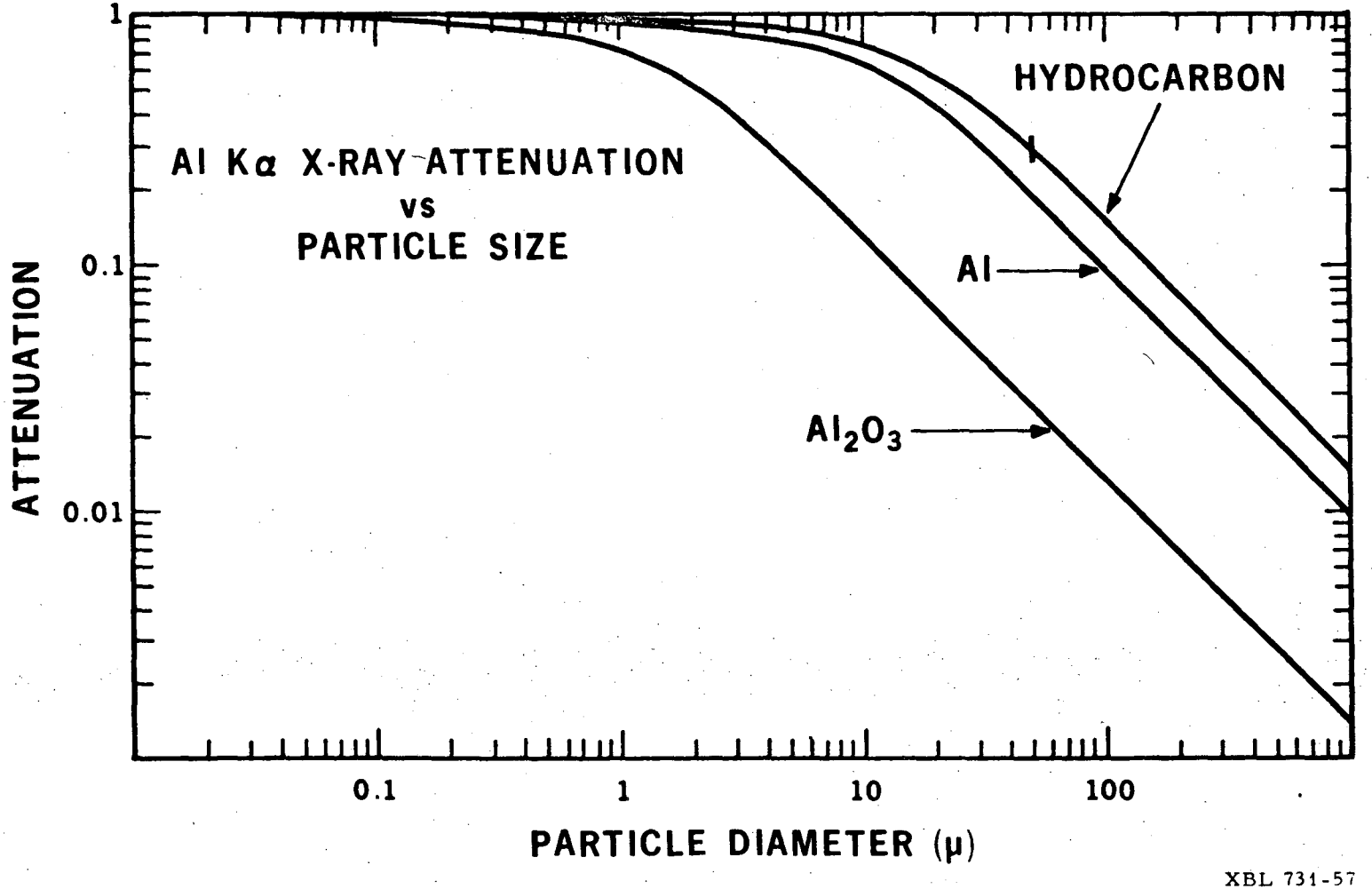
Al Kα X-RAY ATTENUATION
vs
PARTICLE SIZE
HYDROCARBON
Al
Al_2O_3
ATTENUATION
1
0.1
0.01
0.1
1
10
100
PARTICLE DIAMETER (μ)
XBL 731-57

FIG. 14

TECHNICAL INFORMATION DIVISION
LAWRENCE BERKELEY LABORATORY
UNIVERSITY OF CALIFORNIA
BERKELEY, CALIFORNIA 94720